Article:
Mitseas, I.P. orcid.org/0000-0001-5219-1804, Ni, P., Fragkoulis, V.C. et al. (1 more author) (2024) Survival probability surfaces of hysteretic fractional order structures exposed to non-stationary code-compliant stochastic seismic excitation. Engineering Structures, 318. 118755. ISSN: 0141-0296

https://doi.org/10.1016/j.engstruct.2024.118755

Survival probability surfaces of hysteretic fractional order structures exposed to non-stationary code-compliant stochastic seismic excitation

Ioannis P. Mitseas[1,2,*], Peihua Ni[3], Vasileios C. Fragkoulis[4], Michael Beer[5,6,7]

[1] *School of Civil Engineering, University of Leeds, Leeds LS2 9JT, UK*
[2] *School of Civil Engineering, National Technical University of Athens, Iroon Polytechneiou 9, Zografou, Athens 15780, Greece*
[3] *Department of Civil and Environmental Engineering, National University of Singapore, 1 Engineering Drive 2, Singapore 117576, Singapore*
[4] *Department of Civil and Environmental Engineering, University of Liverpool, Liverpool L69 3GH, UK*
[5] *Institute for Risk and Reliability, Leibniz Universität Hannover, Callinstr. 34, Hannover 30167, Germany*
[6] *Institute for Risk and Uncertainty, and School of Engineering, University of Liverpool, Liverpool L69 7ZF, UK*
[7] *International Joint Research Center for Resilient Infrastructure & International Joint Research Center for Engineering Reliability and Stochastic Mechanics, Tongji University, Shanghai 200092, China*

Abstract

A novel first-passage probability stochastic incremental dynamics analysis (SIDA) methodology tailored for hysteretic fractional order structural systems under a fully non-stationary seismic excitation vector consistently designated with contemporary aseismic codes provisions (e.g., Eurocode 8) is developed. Specifically, the vector of the imposed seismic excitations is characterized by evolutionary power spectra that stochastically align with aseismic codes elastic response acceleration spectra, defined for specified modal damping ratios and scaled ground accelerations. Leveraging the concepts of stochastic averaging and statistical linearization, the approximative non-stationary response displacement joint probability density function (PDF) is derived, retaining the particularly coveted attribute of computational efficacy. Subsequently, the coupling with the survival probability model allows for the efficient determination of the

*I.Mitseas@leeds.ac.uk

response first-passage time probability density surfaces and the survival probability surfaces across various limit-state rules and scalable intensity measures. The first-passage time probability serves as a robust engineering demand parameter, effectively monitoring structural behaviour by considering both intensity and timing information, while inherently aligned with pertinent limit-state requirements. Notably, the associated low computational cost and the ability to handle a wide range of complex nonlinear/hysteretic structural behaviours, coupled with its compliance with modern aseismic codes, underscore its potential for applications in the fields of structural and earthquake engineering. A nonlinear system endowed with fractional derivative elements is used to exemplify the method's reliability. The accuracy of the proposed method is validated in a Monte Carlo-based context, conducting nonlinear response time-history analyses with an extensive ensemble of accelerograms compatible with Eurocode 8 response acceleration spectra.

Keywords: Nonlinear stochastic structural dynamics; Fractional order structures; First-passage problem; Aseismic codes; Stochastic averaging; Performance-based earthquake engineering

1 Introduction

In the discipline of structural engineering, encountering the phenomenon of hysteresis is a common occurrence. This fact brings to the fore the critical importance of accurately representing structural systems by thoroughly considering the underlying nonlinear mechanisms governing their behaviour (e.g., [1, 2]). Since in structural applications the dynamic loading to which hysteretic systems are subjected is often random in nature, a proper quantitative treatment of the induced uncertainties becomes a fundamental prerequisite for any aspiring research effort aiming to the assessment of related systems performance (e.g., [3, 4, 5, 6]). Notably, integer order derivative models have predominantly been used to represent systems servicing ordinary structural modelling needs, however, the continually increasing demands for more sophisticated modelling dictate a paradigm shift towards more versatile and advanced mathematical tools, such as fractional calculus [7, 8]. In this setting, several fractional calculus approaches with different attributes can be found in the literature (e.g., [9, 10, 11, 12]). Allowing for an enhanced incorporation of memory effects and long-range dependencies in the system

behaviour, fractional derivative operators have a broad range of engineering applications, spanning from solid mechanics (e.g., [13, 14]) to mechanical engineering (e.g., [15, 16]). This memory-persistent feature is particularly relevant in modelling complex systems with non-local and hereditary characteristics, such as those encountered in the structural engineering field (e.g., [17, 18]). Hence, a multitude of research endeavours focusing on seismic isolation (e.g., [19, 20, 21, 22, 23]), vibration control (e.g., [24]) and energy harvesting applications (e.g., [25, 26]) is added to the arsenal of methods and techniques that demonstrate the efficacy of fractional calculus-based models in the field (e.g., [27, 28, 29, 30, 31, 32]). In this setting, the problem of performance determination of systems comprising terms of fractional order under random excitations represents a sustained challenge in the area of contemporary stochastic structural dynamics.

The emerging concept of Performance-Based Engineering (PBE) enables more tailored and targeted structural designs that prioritise specific performance objectives rather than rigidly adhering to conventional building codes and specifications, while considering the innate randomness characterising the induced hazards (e.g., earthquake, wind, tsunami, fire, etc.) (e.g., [33, 34]). Incremental Dynamic Analysis (IDA) is a common tool within PBE which establishes the relationship between usually employed seismic intensity measures (IMs) such as spectral acceleration or peak ground acceleration, with structural responses known as engineering demand parameters (EDPs) (e.g., peak story drift, inter-story drift ratio, etc.) (e.g., [35]). Also, inherent in the philosophy of the PBE is the fragility analysis which involves the determination of the probability of exceedance of specified limit-state rules (LSs) for various values of the IMs. The resulting IDA curves represent the functional relation between IMs and EDPs, providing critical understandings around the structural behaviour, whereas the generated fragility curves serve pertinent reliability needs offering valuable insights into the seismic resilience and vulnerability of structures. However, performing multi-record IDA within a fully stochastic framework which necessitates assessing higher-order statistical quantities surrounding the selected EDP, such as the Probability Density Function (PDF), demands a resource-intensive Monte Carlo Simulation (MCS) approach (e.g., [36]). This process entails generating a particularly large number of IDA curves to ensure a robust statistical characterisation of the EDP. Consequently, conducting successive reliability assessment based on fragility analysis is anticipated to further escalate the already burdensome computational cost, rendering the process even prohibitive for

large scale complex systems.

The back-and-forth twisting pattern observed even in a single-record IDA indicates multiple points satisfaction of the very same limit-state rule which signals the entrance of a structure into a specific limit/damage state. The relevant literature acknowledges the admission of hardening issues, leading to structural resurrection in extreme cases and phenomena like period elongation. However, the complexity of the mathematical entity of IDA curve is clearly intertwined with scaling as well as timing ambiguity [37]. The herein work is motivated by the desire to tackle both time and scaling peculiarities within a fully probabilistic framework consistently aligned with PBE specifications, studying the problem through the first-passage lens. The selected EDP of the first-excursion time constitutes an excellent response-related variable which performs structural monitoring considering intensity, as well as timing information. In addition, it is naturally coupled with limit state requirements, liberating the potential researcher from interpreting complex twisting patterns behaviour as conforming or non-conforming with a particular performance level. In this context, developing a first-passage time probability stochastic incremental dynamics analysis (SIDA) methodology for systems comprising terms of fractional order and exhibiting hysteretic behaviour becomes pertinent. The raised need should not be confronted solely as a theoretical curiosity, since such needs may reasonably arise in scenarios of real engineering interest involving combined systems like magnetorheological dampers and isolators with structures which exhibit hysteretic behaviour (e.g., [38]).

In passing, the herein proposed approach can be roughly construed as an extension of the work in [37] to account for hysteretic fractional order structures subjected to fully non-stationary aseismic code-compliant stochastic excitations, extending in that manner the range of the generated volume of information leading to an enhanced exploitation of particular method attributes. In the remainder of this paper, Sections 2.1 to 2.4 provide an overview of the mathematical foundations underpinning the developed framework. Section 2.5 offers relevant insights into the intriguing attributes and practical applications of the proposed method. Following this, Section 3 demonstrates the application of the framework through an illustrative example involving a hysteretic structural system comprising fractional derivative elements subjected to Eurocode 8 elastic design spectra. The accuracy of the proposed technique is assessed by juxtaposing the derived results with pertinent MCS data following nonlinear response time-history analysis (RHA).

Finally, Section 4 summarises the main conclusions drawn from the herein study.

2 Mathematical formulation

This section exemplifies the mathematical details involved in the development of the proposed efficient first-excursion PDF-based SIDA methodology. Particular attention has been given on elucidating the various simplifications and assumptions made in the light of numerical efficiency. To ensure the coherency in presenting the theoretical background material without sacrificing the readability of the manuscript, a brief introduction including only the salient concepts associated with the generation of response spectrum compatible stochastic processes is given in Appendix A, whereas the imposed Eurocode 8 elastic design spectra are shown in the following Appendix B.

2.1 Nonlinear structural system comprising fractional derivative elements

The equation governing the dynamics of a quiescent single-degree-of-freedom (SDOF) nonlinear system with fractional derivative elements and base-excited by a non-stationary stochastic seismic acceleration process, is given by

$$\ddot{x}(t) + \beta \mathcal{D}_{0,t}^{\alpha} x(t) + g(t, x, \dot{x}) = \ddot{x}_g(t). \tag{1}$$

In Eq. (1), x denotes the system response displacement and a dot over a variable represents differentiation with respect to time t. $\mathcal{D}_{0,t}^{\alpha}(\cdot)$ accounts for the Caputo fractional derivative operator of order $\alpha \in (0, 1)$, defined as

$$\mathcal{D}_{0,t}^{\alpha} x(t) = \frac{1}{\Gamma(1-\alpha)} \int_0^t \frac{\dot{x}(\tau)}{(t-\tau)^{\alpha}} \, \mathrm{d}\tau, \tag{2}$$

where $\Gamma(\cdot)$ is the Gamma function. Further, β denotes a damping coefficient which is equal to $2\zeta_0 \omega_0^{2-\alpha}$, with ω_0 denoting the natural frequency of the associated linear oscillator and ζ_0 the corresponding damping ratio. Finally, $g(t, x, \dot{x})$ is a nonlinear function which may also describe the hysteretic behaviour of the system whereas $\ddot{x}_g(t)$ stands for a non-stationary stochastic seismic excitation process. The latter is described by an evolutionary power spectrum (EPS) $G(\omega, \zeta_0, t; a_g^s)$, compatible with a target

pseudo-acceleration response spectrum $S(\omega, \zeta_0; a_g^s)$, with a_g^s denoting the scaled images of the seismic excitation intensity. In the ensuing analysis and without sacrificing generality and coherence, the technique proposed in [39] is applied to generate the excitation EPS $G(\omega, \zeta_0, t; a_g^s)$ in alignment with $S(\omega, \zeta_0; a_g^s)$. A concise presentation of the fundamental concepts is provided in Appendix A. It is noted that various techniques have been proposed over the years for deriving power spectra compatible with a given elastic response spectrum typically found in the provisions of modern seismic codes (e.g., Eurocode 8, Chinese GB 50011-2001); some indicative references include [40, 39, 41, 42, 43, 44, 45, 46, 47].

2.2 Determination of the equivalent linear system following a statistical linearization and stochastic averaging approach

Next, aiming at determining the non-stationary response amplitude probability density function (PDF) of the SDOF system in Eq. (1), a linearization treatment of the system is adopted. Specifically, this consists in employing the standard statistical linearization methodology [48], in conjunction with a stochastic averaging treatment [49].

Considering that the system in Eq. (1) is lightly damped, it can be assumed that its response follows a pseudo-harmonic behaviour [49], described by

$$x(t) = A(t)\cos\left(\omega\left(A(t)\right)t + \psi(t)\right), \tag{3}$$

where $A(t) = A$ and $\psi(t) = \psi$ represent the system response amplitude and phase, respectively, whilst $\omega\left(A(t)\right)$ accounts for the equivalent natural frequency of the system. Considering that the processes $A(t)$ and $\psi(t)$ are slowly varying with respect to time, it can be further assumed that they are both constant over one cycle of oscillation roberts1986stochastic. Further, manipulating Eq. (3), the latter two processes are given by [50]

$$A^2(t) = x^2(t) + \left(\frac{\dot{x}(t)}{\omega(A)}\right)^2 \tag{4}$$

and

$$\psi(t) = -\omega(A)t - \arctan\left(\frac{\dot{x}(t)}{x(t)\omega(A)}\right), \tag{5}$$

respectively. In order to facilitate the treatment of the fractional derivative term in Eq. (1), the term

$$h_0(t, x, \mathcal{D}^{\alpha}_{0,t}x, \dot{x}) = \beta\mathcal{D}^{\alpha}_{0,t}x(t) + g(t, x, \dot{x}) - \beta_0\dot{x}(t) \tag{6}$$

is introduced into the SDOF system [51, 52]. Eq. (1) is then recast into

$$\ddot{x}(t) + \beta_0\dot{x}(t) + h_0(t, x, \mathcal{D}^{\alpha}_{0,t}x, \dot{x}) = \ddot{x}_g(t), \tag{7}$$

where $\beta_0 = 2\zeta_0\omega_0$ denotes a damping coefficient. Applying the statistical linearization methodology, the system in Eq. (7) is approximated by an equivalent linear one

$$\ddot{x}(t) + (\beta_0 + \beta(A))\,\dot{x}(t) + \omega^2(A)x(t) = \ddot{x}_g(t), \tag{8}$$

where $\beta(A)$ and $\omega(A)$ represent the amplitude-dependent equivalent linear damping and frequency elements, respectively. The next step of the linearization process consists in minimising the difference formed between Eqs. (7) and (8). Specifically, employing a mean-square minimization of the difference leads to [52]

$$\beta(A) = -\beta_0 + \frac{S(A)}{A\omega(A)} + \beta\omega^{\alpha-1}(A)\sin\left(\frac{\alpha\pi}{2}\right), \tag{9}$$

where

$$S(A) = -\frac{1}{\pi}\int_0^{2\pi} g(A\cos\phi, -A\omega(A)\sin\phi)\sin\phi\ \mathrm{d}\phi \tag{10}$$

with $\phi(t) = \omega(A)t + \psi$, and

$$\omega^2(A) = \frac{F(A)}{A} + \beta\omega^{\alpha}(A)\cos\left(\frac{\alpha\pi}{2}\right) \tag{11}$$

with

$$F(A) = \frac{1}{\pi}\int_0^{2\pi} g(A\cos\phi, -A\omega(A)\sin\phi)\cos\phi\ \mathrm{d}\phi. \tag{12}$$

To further simplify the derivation of the non-stationary response amplitude PDF, the amplitude-dependent equivalent linear elements in Eqs. (9) and (11) are subsequently approximated by equivalent time-dependent ones [52, 27]. To this aim, the time-varying mean values for the equivalent linear elements are determined by taking expectations on Eqs. (9) and (11). This leads to

$$\beta_{eq}(t) = \int_0^{\infty} \beta(A)p(A, t)\ \mathrm{d}A \tag{13}$$

and

$$\omega_{eq}^2(t) = \int_0^\infty \omega^2(A) p(A,t)\ \mathrm{d}A, \tag{14}$$

where $p(A,t)$ represents the non-stationary response amplitude PDF. Considering next Eqs. (13) and (14), Eq. (8) is written as

$$\ddot{x}(t) + (\beta_0 + \beta_{eq}(t))\,\dot{x}(t) + \omega_{eq}^2(t) x(t) = \ddot{x}_g(t), \tag{15}$$

which represents the time-dependent linear system equivalent to the system in Eq. (8).

It is readily seen that $p(A,t)$ is required for the calculation of the time-varying linear elements $\beta_{eq}(t)$ and $\omega_{eq}^2(t)$ in Eqs. (13) and (14). This is attained by employing a stochastic averaging treatment. Specifically, the stochastic differential equation governing the slowly varying response amplitude process is constructed and the associated Fokker-Planck equation is formulated [49, 52]

$$\begin{aligned}\frac{\partial p(A,t)}{\partial t} =& -\frac{\partial}{\partial A}\left\{\left[-\frac{1}{2}(\beta_0+\beta_{eq}(t))A + \frac{\pi G\left(\omega_{eq}(t),\zeta_0,t;a_g^s\right)}{2\omega_{eq}^2(t)A}\right]p(A,t)\right\} \\ &+ \frac{1}{4}\frac{\partial}{\partial A}\left\{\frac{\pi G\left(\omega_{eq}(t),\zeta_0,t;a_g^s\right)}{\omega_{eq}^2(t)}\frac{\partial p(A,t)}{\partial A}\right. \\ &\left.+ \frac{\partial}{\partial A}\left(\frac{\pi G\left(\omega_{eq}(t),\zeta_0,t;a_g^s\right)}{\omega_{eq}^2(t)}p(A,t)\right)\right\}.\end{aligned} \tag{16}$$

A solution to Eq. (16) for the particular case of linear SDOF systems with fractional derivative elements subject to non-stationary excitation has been proposed in [52], namely

$$p(A,t) = \frac{JA}{c(t)}\exp\left(-\frac{JA^2}{2c(t)}\right), \tag{17}$$

where

$$J = \omega_0^{\alpha-1}\sin\left(\frac{\alpha\pi}{2}\right) \tag{18}$$

and $c(t)$ is a time-dependent coefficient to be determined [27, 53]. A closed form expression for the latter is derived by substituting Eq. (17) into Eq. (16)

and manipulating. This leads to the first-order nonlinear ordinary differential equation

$$\dot{c}(t) = -\left[\beta_0 + \beta_{eq}(c(t))\right] c(t) + J\pi \frac{G\left(\omega_{eq}(c(t)), \zeta_0, t; a_g^s\right)}{\omega_{eq}^2(c(t))}, \tag{19}$$

which can be readily solved by applying any suitable numerical scheme, such as the 4th order Runge-Kutta method. Thus, Eqs. (17) to (19), and Eqs. (13) and (14) define a set of equations used for determining the response amplitude PDF and the equivalent linear elements corresponding to the nonlinear system in Eq. (1). In passing, it is noted that the time-dependent function $c(t)$ is also used to compute the non-stationary response variance of the SDOF system, which is approximated by [52]

$$\mathrm{E}[x^2] = J^{-1} c(t). \tag{20}$$

2.3 Non-stationary transition and joint response amplitude PDF determination

A closed-form expression for the non-stationary transition response amplitude PDF has been recently proposed in [53] for SDOF nonlinear systems with fractional derivative elements. In this regard, considering the target system in Eq. (1) one gets

$$p(A_2, t_2 | A_1, t_1) = \frac{JA_2}{c(t_1, t_2)} \exp\left(-J\frac{A_2^2 + h^2(t_1, t_2)}{2c(t_1, t_2)}\right) I_0\left(\frac{JA_2 h(t_1, t_2)}{c(t_1, t_2)}\right), \tag{21}$$

where $c(t_1, t_2)$ and $h(t_1, t_2)$ represent a set of unknown time-dependent functions, and $I_0(\cdot)$ denotes the modified Bessel function of the first kind of zero order [54]. Following closely the presentation in [53], the time-dependent functions $c(t_1, t_2)$ and $h(t_1, t_2)$ are determined by solving the differential equations

$$\frac{\mathrm{d}c(t_1, t_2)}{\mathrm{d}t_2} + \left(\beta_0 + \beta_{eq}(t_1, t_2)\right) c(t_1, t_2) - \pi J \, \frac{G\left(\omega_{eq}(t_1, t_2), \zeta_0, t_2; a_g^s\right)}{\omega_{eq}^2(t_1, t_2)} = 0 \tag{22}$$

and

$$\frac{\mathrm{d}h(t_1, t_2)}{\mathrm{d}t_2} + \frac{1}{2}\left(\beta_0 + \beta_{eq}(t_1, t_2)\right) h(t_1, t_2) = 0, \tag{23}$$

where β_{eq} and ω_{eq}^2 are the time-dependent equivalent elements in Eqs. (13) and (14), respectively, and $G\left(\omega_{eq}(t_1,t_2),\zeta_0,t_2;a_g^s\right)$ is the EPS compatible with the target pseudo-acceleration response spectrum.

Finally, adopting a Markovian response assumption for the amplitude process, and also considering the initial condition $p(A_2,t_2|A_1,t_1)=\delta(A_2-A_1)$, with $\delta(\cdot)$ denoting the Dirac delta function, in conjunction with Eqs. (17) and (21), it was proved in [53] that the joint response amplitude PDF is given by

$$\begin{aligned} p(A_1,t_1;A_2,t_2) =& \frac{J^2A_1A_2}{c(t_1)c(t_1,t_2)}I_0\left(\frac{JA_2h(t_1,t_2)}{c(t_1,t_2)}\right) \\ & \times\exp\left(-J\frac{A_2^2c(t_1)+A_1^2c(t_1,t_2)+h^2(t_1,t_2)c(t_1)}{2c(t_1,t_2)}\right). \end{aligned} \tag{24}$$

The interested reader may resort to [53, 55, 56] for a detailed derivation of the joint response amplitude PDF in Eq. (24).

2.4 Hysteretic system limit-state rule first-passage time density surfaces and survival SIDA probability surfaces determination

In this section, the first-passage problem pertaining to the target system in Eq. (1) is considered. In this regard, the probability of first-passage is defined as the probability that the response amplitude $A(t)$ crosses a pre-set barrier B corresponding to a limit state, for the first time over the time interval $[0,T]$. Hence, the survival probability $P_B(T,A(t);a_g^s)$ of the system is defined as the probability that the response amplitude stays below the pre-set limit state over $[0,T]$. Next, the time interval $[0,T]$ is discretised into a subset of time intervals as [57, 53]

$$[0,T]=\bigcup_{i=1}^{N}[t_{i-1},t_i], \tag{25}$$

with $t_0=0$ and $t_N=T$. The step of the time interval discretisation (e.g., [58]) is taken equal to $t_i=t_{i-1}+\ell T_{eq}(t_{i-1})$, with $\ell\in(0,1]$ and $T_{eq}(t)=\frac{2\pi}{\omega_{eq}(t)}$ denoting the time-dependent equivalent natural period.

Further, exploiting the slow variation of the response amplitude $A(t)$ (see related discussion in Section 2.2), it is assumed that $A(t)$ and thus $P_B(T,A(t);a_g^s)$ remain constant within each of the intervals defined in Eq. (25).

The survival probability of the target system in Eq. (1) is approximated over the sub-intervals $[t_{i-1}, t_i]$, $i = 1, \cdots, N$, by [57, 53]

$$P_B(T, A(t); a_g^s) = \prod_{i=1}^{N} (1 - P_i), \tag{26}$$

where P_i accounts for the first excursion probability of the response amplitude within $[t_{i-1}, t_i]$, given that no previous crossing of the limit state B has occurred for $t < t_{i-1}$. Further, taking into account the Markovian property for the response amplitude as well as the mathematical definition of the conditional probability, the calculation of the first excursion probability $P_i, i = 1, 2, \ldots, N$, simplifies to [57, 53]

$$P_i = \frac{Prob\{(A(t_i) \geq B) \cap (A(t_{i-1}) < B)\}}{Prob\{A(t_{i-1}) < B\}} = \frac{Q_{i-1,i}}{H_{i-1}}, \tag{27}$$

with

$$Q_{i-1,i} = \int_B^\infty \mathrm{d}A_i \int_0^B p(A_{i-1}, t_{i-1}; A_i, t_i)\ \mathrm{d}A_{i-1} \tag{28}$$

and

$$H_{i-1} = \int_0^B p(A_{i-1}, t_{i-1})\ \mathrm{d}A_{i-1}. \tag{29}$$

Clearly, the calculation of the survival probability in Eq. (26) relies on the computation of the integrals in Eqs. (28) and (29) which, in turn, depends on computing the joint response amplitude PDF in Eq. (24). This is done in two steps. First, considering that the time-dependent equivalent elements $\omega_{eq}(t)$ and $\beta_{eq}(t)$ (see Eqs. (13) and (14)) are slowly varying in time and thus constant over each sub-interval $[t_{i-1}, t_i]$ ($i = 1, 2, \ldots, N$) prompts the use of the theory of locally stationary processes (e.g., [59, 60]). In this context, the differential equations Eqs. (22) and (23) are solved over $[t_{i-1}, t_i]$ leading to

$$c(t_{i-1}, t_i) = J\pi\ \frac{G\left(\omega_{eq}(t_{i-1}), \zeta_0, t_{i-1}; a_g^s\right)}{\omega_{eq}^2(t_{i-1})}\ \tau_i \tag{30}$$

and

$$h(t_{i-1}, t_i) = A_{i-1}\sqrt{1 - (\beta_0 + \beta_{eq}(t_{i-1}))\tau_i}, \tag{31}$$

respectively, with $\tau_i = t_i - t_{i-1}$. Then, employing elements of the theory of Bessel functions [54], Eq. (24) is recast into

$$\begin{aligned} p(A_{i-1}, t_{i-1}; A_i, t_i) =& \frac{J^2 A_{i-1} A_i}{c(t_{i-1}) c(t_i)(1-r_i^2)} \; I_0 \left(\frac{J A_{i-1} A_i r_i}{\sqrt{c(t_{i-1}) c_i(t) \left(1-r_i^2\right)^2}} \right) \\ & \times \exp\left(-J \frac{A_i^2 c(t_{i-1}) + A_{i-1}^2 c(t_i)}{2 c(t_{i-1}) c(t_i) \left(1-r_i^2\right)^2} \right), \end{aligned} \tag{32}$$

where

$$r_i^2 = \frac{c(t_{i-1})}{c(t_i)} \left[1 - \left(\beta_0 + \beta_{eq}(t_{i-1}) \right) \tau_i \right]. \tag{33}$$

Finally, substituting Eq. (32) into Eq. (28) while also taking into account Eqs. (30) and (31), yields

$$Q_{i-1,i} = D_0 + \sum_{m=1}^{M} D_m, \tag{34}$$

where

$$D_0 = (1-r_i^2) \exp\left(-\frac{JB^2}{2c(t_i)(1-r_i^2)} \right) \left[1 - \exp\left(-\frac{JB^2}{2c(t_{i-1})(1-r_i^2)} \right) \right] \tag{35}$$

and

$$D_m = \frac{r_i^{2m} J^{2m+2}}{\left(c(t_{i-1}) c(t_i) \right)^{m+1} \left(1-r_i^2\right)^{2m+1} \prod_{k=1}^{m} (2k)^2} L_m. \tag{36}$$

The term L_m in Eq. (36) is defined as

$$\begin{aligned} L_m = \; & 4^m \left(1-r_i^2\right)^{2m+2} \left[c\left(t_{i-1}\right) c\left(t_i\right) \right]^{m+1} J^{-2m-2} \; \Gamma\left(m+1, \frac{JB^2}{2c(t_i)(1-r_i^2)} \right) \\ & \times \left[\Gamma(m+1) - \Gamma\left(m+1, \frac{JB^2}{2c(t_{i-1})(1-r_i^2)} \right) \right], \end{aligned} \tag{37}$$

where $\Gamma(z_1, z_2) = \int_{z_2}^{\infty} s^{z_1 - 1} \mathrm{e}^{-s} \mathrm{d}s$ is the upper incomplete Gamma function [54]. In a similar manner, substituting Eq. (21) into Eq. (29) and manipulating leads to

$$H_{i-1} = 1 - \exp\left(-\frac{JB^2}{2c(t_{i-1})} \right). \tag{38}$$

Hence, considering Eqs. (34) and (38), the first excursion probability for the interval $[t_{i-1}, t_i]$ $(i = 1, 2, \ldots, N)$ is computed by Eq. (27), which is then used to calculate the survival probability of the target system by employing Eq. (26). In this setting, the first-passage time PDF is obtained by

$$p_B\left(T, A(t); a_g^s\right) = -\frac{\mathrm{d}P_B\left(T, A(t); a_g^s\right)}{\mathrm{d}T}. \tag{39}$$

A detailed derivation of Eqs. (27) to (39) can be found in [61, 55, 57, 53].

2.5 Definition of limit-state rules and mechanisation of the proposed methodology

The existing body of literature employs limit-state rules, often defined in relation to overall system inelastic deformation or maximum inter-story drift, as seen in previous studies (e.g., [62, 63]). However, in the current study, a distinctive perspective is adopted by examining the problem through the lens of the first-passage analysis (e.g., [64, 37, 65]). This is achieved by selecting the response limit-state first-excursion time as the EDP. Given the alternative nature of the chosen EDP, the proposed PDF-based SIDA methodology establishes a functional relationship between IMs and EDPs, in conjunction with LSs. At this point, it should be recalled that the standard IDA technique is concerned with the estimation of the relation between IMs and EDPs whereas it requires an additional careful handling of the coupling with the LSs for interpreting potential conformity with a particular performance level. In Table 1, a potential mapping between performance requirements and system limit-states, expressed in terms of inter-story drift for a typical structure is provided.

Table 1. Performance requirements and limit states.

Limit states	Limit-state barrier B
Impaired function	4.0×10^{-2}
Life safety	5.0×10^{-2}
Onset of collapse	6.5×10^{-2}

The mechanisation of the proposed response first-passage PDF-based stochastic IDA methodology comprises the following steps:

1. Derive a compatible excitation EPS $G(\omega, \zeta_0, t; a_g^s)$ with a given pseudo-acceleration response spectrum for a scaled picture of the peak ground acceleration a_g^s by following the approach in Appendix A; see [39] for more details.
2. Following the stochastic averaging and linearization treatment presented in Section 2.2, solve numerically Eq. (19) to compute $c(t)$, while also considering the time-dependent equivalent elements in Eqs. (13) and (14). Then, compute the response amplitude PDF $p(A, t)$ by employing Eqs. (17) and (18).
3. Define a barrier B and following Section 2.4 determine the first-passage time PDF for the associated limit state. Subsequently, evaluate the survival probability and first-passage time PDF by Eqs. (26) and (39), respectively.
4. Repeat steps 1-3 for the scaled images of the peak ground acceleration a_g^s to define the survival SIDA probability surfaces and the response first-passage time probability density surfaces considering the various limit states.

2.6 Discussion on aspects of the proposed methodology

This section provides an exploration of several key aspects, encompassing the advantages, limitations and potential practical applications of the proposed framework. In comparison to the state-of-the-art methodologies available in the literature, the proposed first-passage PDF-based SIDA methodology for hysteretic fractional order structural systems bears several significant and intriguing features which are summarised in the following: (i) it accommodates nonlinear structural systems exhibiting hysteretic behaviour; (ii) the methodology addresses complex and more sophisticated modelling requirements resorting to fractional calculus concepts. This element makes it particularly appealing especially considering the particular volume of current research efforts in the ever-changing and interdisciplinary field of engineering mechanics which employ such modelling concepts (e.g., [13, 14, 15, 16, 17, 18, 20, 23, 19, 27, 28, 24, 29]); (iii) the ground motion is represented as a vector of aseismic code-compliant fully non-stationary stochastic processes, rather

than a set of scaled earthquake records (e.g., Multi-record IDA), eliminating the potential bias in selecting and scaling specific ground motion records. This is particularly pertinent given the ongoing controversy in the literature regarding this issue (e.g., [66]); (iv) the methodology significantly reduces the bias introduced by the selection of a limited number of seismic motion records, typically around seven (e.g., [2]); (v) the methodology is built on the provision of higher order statistics, around the selected EDP, rather than relying solely on mean and standard deviation estimates, as is currently the norm in the literature; (vi) it addresses timing as well as intensity peculiarities, employing an innovative limit-state first-passage time as an EDP, curing in that manner the necessity to deal with intricate and convoluted patterns of IDA curves related with typically employed EDPs (e,g, inter-story drifts); (vii) the proposed framework is considerably less computationally demanding compared to nonlinear response history analysis (RHA) for compatible ground motion records. Certainly, employing a conventional brute force implementation of the IDA methodology for determining higher order EDP statistics within a Monte-Carlo based context can pose significant computational challenges, rendering the process even prohibitive for large scale complex systems; (viii) the methodology provides with the response first-passage time probability density surfaces instead of the conventional IDA curves found in a number of pertinent studies in the field. Notably, the generated surfaces encompass information on both timing and excitation intensity. Moreover, the presented survival SIDA probability surfaces cater for a higher volume of information as compared with their counterpart in PBE analysis, namely that of fragility curves. It is noteworthy that an intersection over a survival probability surface along the seismic acceleration axis leads to a form which bears high resemblance with the standard definition of fragility curves, as is typically encountered in the literature. Interestingly, an intersection along the time axis provides with the time-evolving survival probability for a particular excitation level. These observations confirm that the two generated types of surfaces could serve practical needs, operating complementary to well-established concepts as the ones mentioned above, thus attracting a particular interest in the structural field; (ix) it provides with stochastically derived time-varying forced vibrational system properties thus offering a solid basis for interpreting the dynamic character of the system. Note that this significant operation cannot be determined following typical nonlinear RHA; (x) it employs an innovative EDP, which inherently couples IM, EDP, and LS attributes. Notably, this contrasts with the standard IDA technique,

which typically requires additional handling of the subsequent coupling with LSs for interpreting potential conformity with a specific performance level. The herein work represents a pioneering effort within the engineering realm, addressing a critical and emerging gap between advanced stochastic engineering dynamics and contemporary design code provisions in conceptual agreement with PBE content. This study aims to reconcile the complexity of sophisticated modelling requirements incorporating concepts from fractional calculus, code-compliant non-stationary excitations, and structural nonlinearities with the practical frameworks used in current structural design and analysis standards. By bridging these advanced theoretical approaches with established engineering practices, the developed methodology seeks to enhance the applicability of modern engineering solutions for current and future structural related needs. Relevant remarks should be included regarding the expected levels of accuracy for the developed method, since it incorporates various techniques for efficiency, each with potential limitations. The integration of stochastic averaging and statistical linearization methodologies could potentially undermine accuracy in cases of highly nonlinear and low-performance structures. Lastly, the method imposes no restrictions on the excitation process, except for the Gaussian assumption.

3 Illustrative application

In this section, the proposed response first-passage PDF-based stochastic IDA methodology is numerically exemplified by considering a nonlinear structural system endowed with fractional derivative elements subjected to stochastic seismic excitation in alignment with specifications prescribed by contemporary aseismic codes. The degree of accuracy is assessed by comparisons with pertinent results derived from nonlinear RHA for an ensemble of accelerograms compatible with Eurocode 8 response acceleration spectra (see Appendix B).

3.1 Hysteretic structural system model endowed with fractional derivative elements

The governing equations of the bilinear hysteretic system as well as the pertinent expressions for the time-dependent equivalent linearised elements are derived in C. Note that such system modelling can be reasonably found

in a number of relevant studies in the field of earthquake engineering (e.g., [48, 27]). The following parameter values $\omega_0 = 10\ rad/s$, $\zeta_0 = 0.05$, $\alpha = 0.5$, $\gamma = 0.5$ and $x_y = 0.03\ m$ have been used in the system modelling provided in Eqs. (55) to (62). Further, the Eurocode 8 elastic pseudo-acceleration design spectrum $S(\omega, \zeta_0; a_g^s)$ for soil type B is selected as the baseline spectrum for generating the input spectra $G(\omega, \zeta_0, t; a_g^s)$ following the specifications and the scheme presented in Appendix B and Appendix A, respectively. Note that the use of the latter scheme is not binding, and alternative approaches found in the literature for deriving power spectra compatible with design spectra can be considered as well. Also, it is noteworthy that provisions defined by various aseismic codes can be readily considered by the proposed framework, rendering the current choice of Eurocode 8 non restrictive. The non-stationary attributes of the excitation are modelled through the $\ddot{x}_g^R(t)$ component of Eq. (40) which corresponds to the recorded time history at El Centro site during the SOOE (NS) component of the Imperial Valley earthquake on May 18, 1940 (e.g., [39, 27]). The scaled images for the induced excitation are determined as $a_g^s = g \times [0.4, 0.6, 0.8, 1.0, 1.2]$, while the considered limit-state rules are shown in Table 1. The proposed methodology requires first the determination of the design spectrum compatible evolutionary power spectra $G(\omega, \zeta_0, t; a_g^s)$ for the above mentioned scaled acceleration intensities a_g^s. Next, the methodology outlined in Section 2.1 to 2.4 enables the efficient determination of the response first-passage time probability density surfaces as well as the survival SIDA probability surfaces for each and every of the considered limit-state barriers B. In Fig. 1 and Fig. 2, the survival SIDA probability and first-passage time PDF surfaces of the hysteretic fractional order system under consideration for the limit-state of "Impaired function" are efficiently determined and compared with the corresponding MCS data. Notably, targeted comparisons related to both the lower and upper excitation intensity bounds have been included as well, showcasing the achieved degree of accuracy of the proposed methodology.

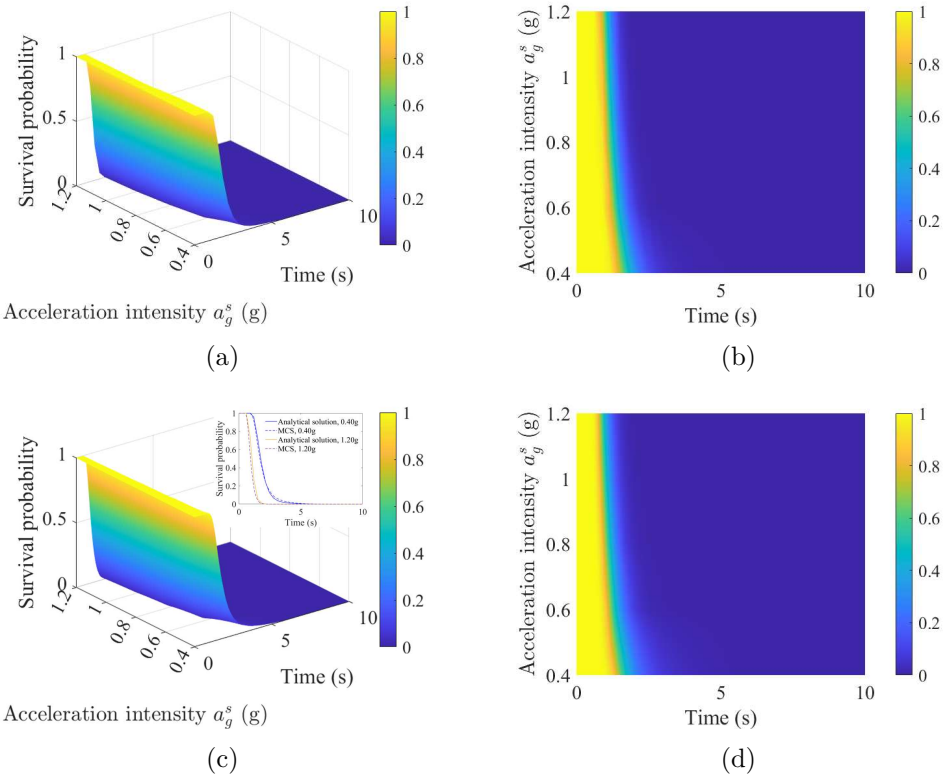

Fig. 1. Survival SIDA probability surface estimates for the bilinear hysteretic fractional order system for the limit state "Impaired function": (a) Proposed analytical solution (3D); (b) Proposed analytical solution (2D); (c) MCS estimates (3D); (d) MCS estimates (2D) (10, 000 realisations).

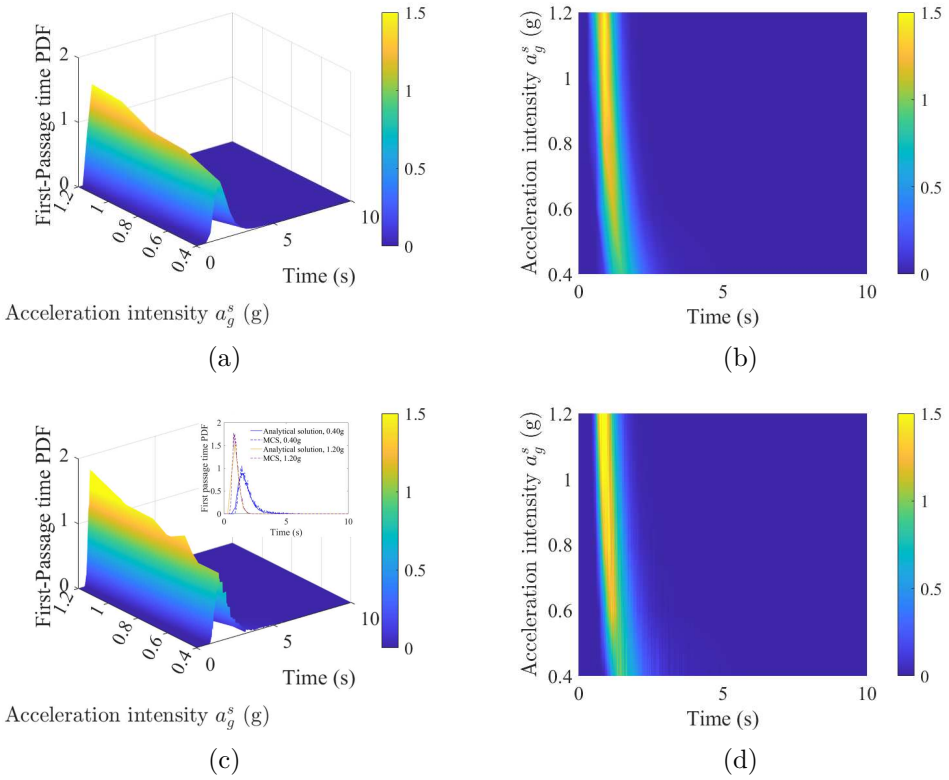

Fig. 2. Response first-passage time probability density surface estimates for the bilinear hysteretic fractional order system for the limit state "Impaired function": (a) Proposed analytical solution (3D); (b) Proposed analytical solution (2D); (c) MCS estimates (3D); (d) MCS estimates (2D) (10,000 realisations).

Next, in Figs. (3-6), pertinent results considering the limit-states of "Life safety" and "Onset of Collapse" are presented.

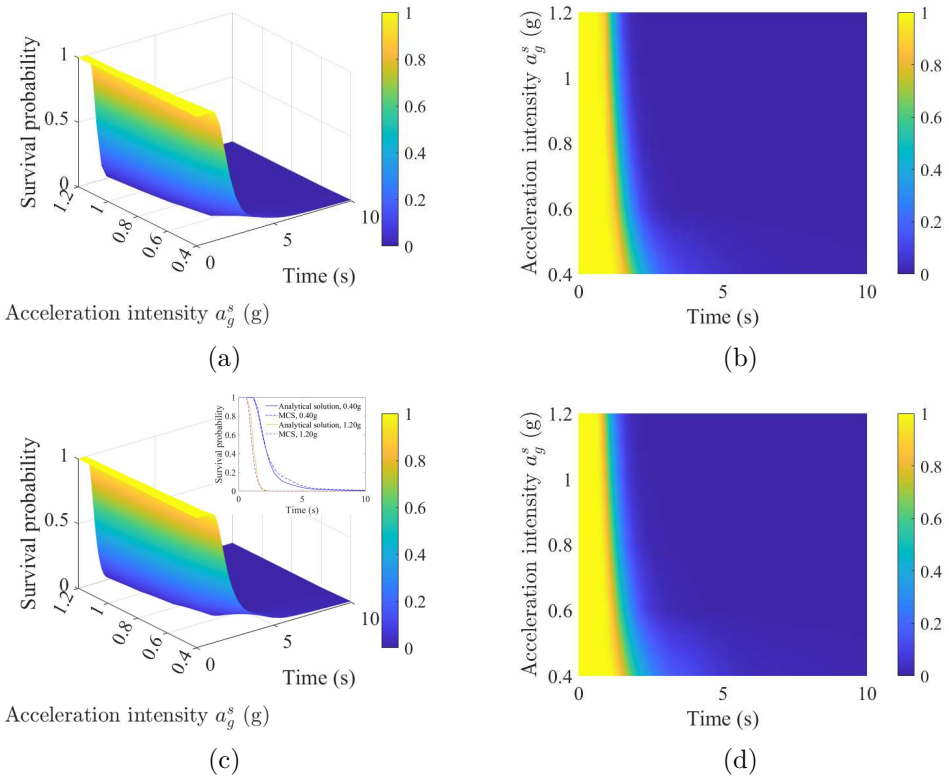

Fig. 3. Survival SIDA probability surface estimates for the bilinear hysteretic fractional order system for the limit state "Life safety": (a) Proposed analytical solution (3D); (b) Proposed analytical solution (2D); (c) MCS estimates (3D); (d) MCS estimates (2D) (10,000 realisations).

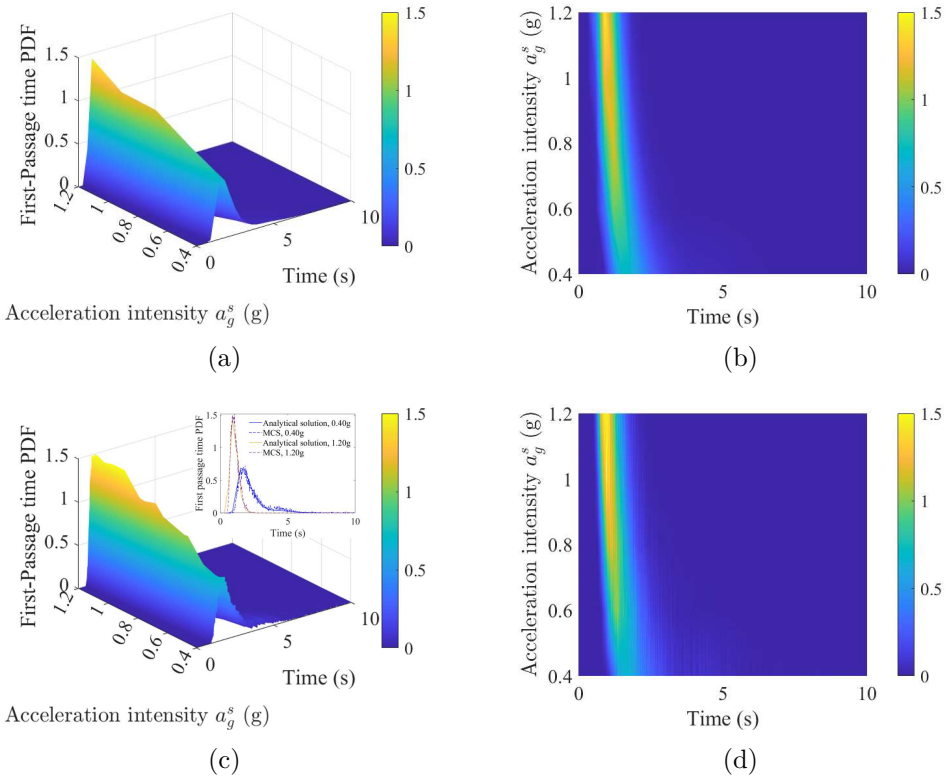

Fig. 4. Response first-passage time probability density surface estimates for the bilinear hysteretic fractional order system for the limit state "Life safety": (a) Proposed analytical solution (3D); (b) Proposed analytical solution (2D); (c) MCS estimates (3D); (d) MCS estimates (2D) (10, 000 realisations).

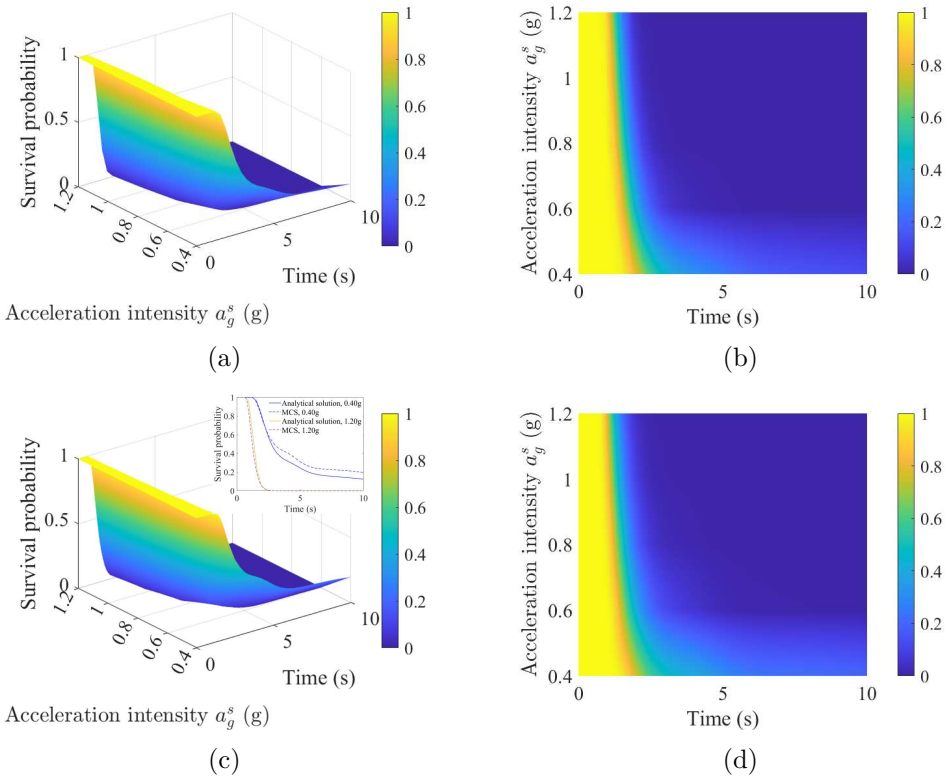

Fig. 5. Survival SIDA probability surface estimates for the bilinear hysteretic fractional order system for the limit state "Onset of collapse": (a) Proposed analytical solution (3D); (b) Proposed analytical solution (2D); (c) MCS estimates (3D); (d) MCS estimates (2D) (10, 000 realisations).

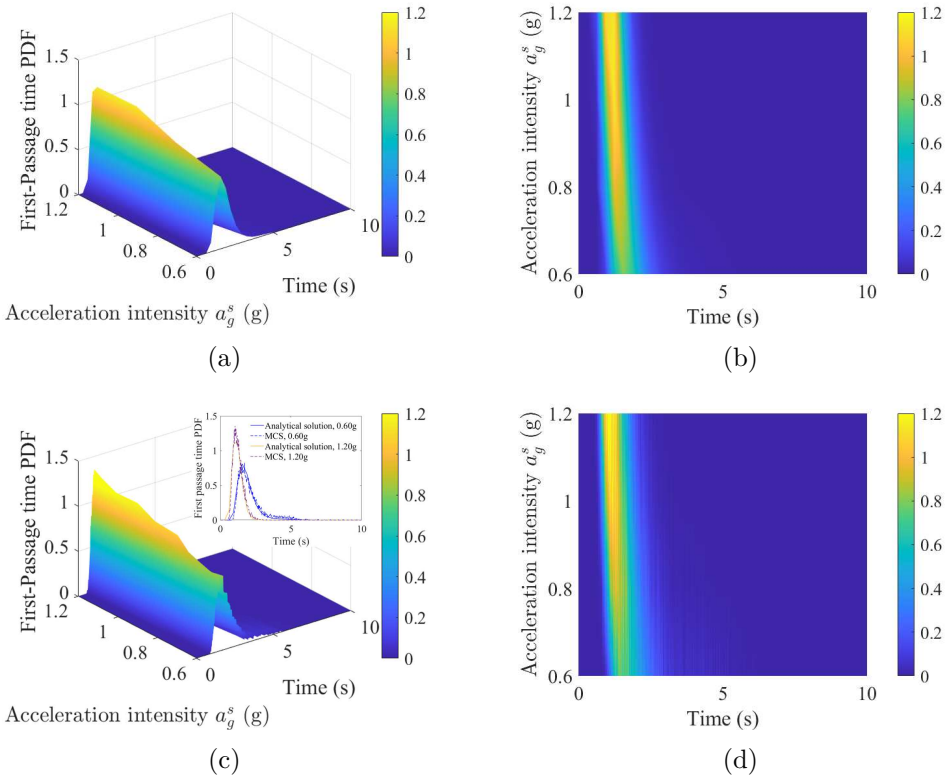

Fig. 6. Response first-passage time probability density surface estimates for the bilinear hysteretic fractional order system for the limit state "Onset of collapse": (a) Proposed analytical solution (3D); (b) Proposed analytical solution (2D); (c) MCS estimates (3D); (d) MCS estimates (2D) (10,000 realisations).

To evaluate the attained accuracy level, comparisons with relevant data from MCS are included in Fig. 1 to Fig. 6. More precisely, the spectral representation method outlined in [67] is employed to create an ensemble of 10,000 acceleration time histories, compatible with the reference seed design spectrum corresponding to the specific scaled image of the excitation a_g^s. Subsequently, the governing equation of motion of the hysteretic fractional order system of Eq. (1) is exposed to the above ensemble of accelerograms and is numerically solved by resorting to an L1-algorithm [19]. Notably, the limit state first-passage time probability density surfaces as well as the survival SIDA probability surfaces are computed with minimal

computational expense, leveraging the capabilities of the proposed stochastic dynamics methodology detailed in Section 2. Evidently, comparisons with MCS data demonstrate a satisfactory degree of accuracy, validating the proposed technique appropriateness for related performance-based engineering applications. The generated limit-state PDF surfaces offer a comprehensive statistical representation of the employed EDP with respect to the excitation intensity. In this setting, deriving other associated statistical quantities, such as the mean and/or the mode is identified as a straightforward task. Notably, considering the modes can lead to an establishment of a desirable one-to-one mapping in the functional relationship between IMs and EDPs, circumventing issues related to complex non-monotonic patterns commonly observed in conventional IDA curves. Another notable aspect of the structural behaviour is that, for higher barriers under low levels of excitation intensity, the survival probability does not decrease to zero as it is observed for the lower barriers. Instead, it reaches a constant non-zero value. Interestingly, this kind of behaviour is noted on Fig. 5. For such cases the concept of the first-passage time probability density function is meaningless (e.g., [68]) leading the corresponding generated first-passage density surface to be defined in an updated excitation intensity range.

It is worth noting that the proposed method considerably reduces the computational workload compared to nonlinear RHA within a MCS framework. To provide with an indicative order of magnitude for the computational expenses involved, using a standard laptop setup (1.9 GHz 4-Core Intel Core i7 processor and 16 GB RAM), the proposed technique typically takes 8-10 min to generate the pertinent outcomes for a single limit-state whereas a MCS-based estimation, utilising $10,000$ time-histories, necessitates around 50 min for addressing the same needs. The low computational cost of the proposed approach renders it potentially a promising analysis tool, particularly for preliminary stochastic reliability analyses of nonlinear fractional order structures. It is worth mentioning that the proposed technique can be easily adapted to accommodate requirements outlined in any current code of practice, addressing a wide range of hazards such as ocean waves, winds, hurricanes, tsunamis, and others.

4 Concluding remarks

This paper proposes a response first-passage time PDF-based stochastic incremental dynamics analysis methodology for hysteretic fractional order structural systems subjected to a fully non-stationary seismic excitation vector consistently designated with contemporary aseismic codes provisions. Resorting to stochastic averaging and statistical linearization concepts, the approximate non-stationary response displacement joint PDF is derived in a straightforward manner, preserving computational efficacy. Following this, the integration with the survival probability model enables the efficient determination of the response first-passage time probability density surfaces and the survival probability surfaces for a scalable intensity measure adhering to different limit-state rules. It is noteworthy that the proposed method utilises an incremental mechanisation, reminiscent to the one used in the standard implementation of IDA. This fact not only ensures compatibility by scaling intensity but also aligns with established practices, enhancing its practicality for adoption in a variety of engineering scenarios. The selected engineering demand parameter of the first-passage time, which indicates a structure entrance into a specific limit/damage state, serves as a valuable response variable for monitoring structural behaviour. It considers both intensity and timing information while it is inherently coupled with limit-state requirements. The methodology departs from the current literature norm, which relies solely on mean and standard deviation estimates, by incorporating higher-order statistics around the selected EDP (e.g. PDFs). Further, the methodology provides with the response first-passage time probability density surfaces instead of the conventional IDA curves. In addition, the generated survival SIDA probability surfaces provide a wealth of information compared to their counterpart in PBE analysis, namely that of fragility curves. Moreover, intersections on a survival probability surface yield to various outcomes of significant engineering interest and practical merit. Equally important is the fact that the methodology addresses the growing need for more sophisticated modelling, advocating a logical shift towards advanced mathematical tools such as fractional calculus. Importantly, the associated low computational cost enhances the appeal and utility of the proposed methodology for related performance-based engineering applications at least on a preliminary design stage. The concepts involved have been numerically illustrated using a bilinear hysteretic fractional order structural system exposed to non-stationary ground motion modelled in accordance with con-

temporary aseismic code provisions. Lastly, a MCS-based nonlinear RHA with a large ensemble of non-stationary accelerograms assess the accuracy of the proposed framework.

Declaration of competing interest

The authors declare that they have no known competing financial interests or personal relationships that could have appeared to influence the work reported in this paper.

Acknowledgment

The authors gratefully acknowledge the support by the Hellenic Foundation for Research and Innovation (Grant No. 1261), by the German Research Foundation (Grant No. FR 4442/2-1), by the National Natural Science Foundation of China (Grant No. 72271025), and by the Guangdong Basic and Applied Basic Research Foundation (Grant No. 2023A1515011532).

A Derivation of design spectrum compatible excitation non-stationary power spectrum

Following closely [39], the non-stationary stochastic excitation $\ddot{x}_g(t)$ in Eq. (1) can be written as

$$\ddot{x}_g(t) = a\ddot{x}_g^R(t) + \varphi(t)\ddot{x}_g^S(t), \tag{40}$$

where $\ddot{x}_g^R(t)$ is a fully non-stationary segment from a real seismic record, with a denoting a scaling coefficient, and $\ddot{x}_g^S(t)$ accounts for a time-modulated quasi-stationary corrective Gaussian process, with $\varphi(t)$ representing a time-modulating function. The latter is given by [69]

$$\varphi(t) = \begin{cases} \left(\frac{t}{t_1}\right)^2, & t < t_1 \\ 1, & t_1 \leq t \leq t_2 \\ \exp\left[-\beta_m(t-t_2)\right], & t > t_2 \end{cases}, \tag{41}$$

where T_s denotes the time window within which the seismic record is assumed to be stationary. Further, $t_2 = t_1 + T_s$, with t_1 and t_2 denoting, respectively,

the time instants when the Husid function [70] is equal to 0.05 and 0.95. Finally, β_m defines the decay of the modulating function.

Next, considering a quiescent linear SDOF system subject to $\ddot{x}_g^R(t)$ and $\ddot{x}_g^S(t)$, and assuming that the corresponding response spectra are $S^R(\omega, \zeta_0; a_g^s)$ and $S^S(\omega, \zeta_0; a_g^s)$, respectively, an approximate relationship for the design spectrum is given by

$$S(\omega, \zeta_0; a_g^s) = \sqrt{a^2 \; S^R\left(\omega, \zeta_0; a_g^s\right)^2 + S^S\left(\omega, \zeta_0; a_g^s\right)^2}. \tag{42}$$

The scaling coefficient in Eq. (42) takes values in $(0, 1]$ and is calculated via

$$a = \min\left\{\frac{S(\omega, \zeta_0, a_g^s)}{S^R(\omega, \zeta_0; a_g^s)}\right\}. \tag{43}$$

Working towards determining $G^S(\omega, \zeta_0; a_g^s)$, a framework based on a combination of an approximate solution treatment of the first-passage time problem [71] and of an iterative scheme [72] is adopted in the following. In this context, first, a relationship between the one-sided power spectrum $G^S(\omega, \zeta_0; a_g^s)$ and the response spectrum $S^S(\omega_0, \zeta_0; a_g^s)$ is established in the form

$$S^S(\omega_0, \zeta_0; a_g^s) = \eta_{x^S} \omega_0^2 \sqrt{\lambda_{0,x^S}(\omega_0, \zeta_0; a_g^s)}. \tag{44}$$

λ_{0,x^S} corresponds to the 0th order stationary response spectral moment of a linear SDOF oscillator with natural frequency ω_0 and damping ratio ζ_0, with the general nth order form given by

$$\lambda_{n,x^S}(\omega_0, \zeta_0; a_g^0) = \int_0^\infty \omega^n \frac{1}{\left(\omega_0^2 - w^2\right)^2 + \left(2\zeta_0\omega_0\omega\right)^2} G^S(\omega, \zeta_0; a_g^0) \; \mathrm{d}\omega. \tag{45}$$

Further, η_{x^S} is the "peak factor" defined as [71]

$$\eta_{x^S}(T_s, p) = \sqrt{2\ln\left(2\mu_{x^S}\left[1 - \exp\left(-\delta_{x^S}^{1.2}\sqrt{\pi \ln(2\mu_{x^S})}\right)\right]\right)}, \tag{46}$$

with

$$\mu_{x^S} = \frac{T_s}{2\pi}\sqrt{\frac{\lambda_{2,x^S}}{\lambda_{0,x^S}}}(-\ln p)^{-1} \quad \text{and} \quad \delta_{\mathrm{x^S}} = \sqrt{1 - \frac{\lambda_{1,\mathrm{x^S}}^2}{\lambda_{0,\mathrm{x^S}}\lambda_{2,\mathrm{x^S}}}} \tag{47}$$

denoting the mean zero crossing rate and the spread factor, respectively. Setting next $p = 0.5$ in Eq. (46) and adopting an approximate expression

for the 0th order stationary response spectral moment (see [71]), Eq. (44) is recast into

$$S^S(\omega_0,\zeta_0;a_g^s)=\eta_{x^S}^2\omega_0 G^S(\omega_0,\zeta_0;a_g^s)\left(\frac{\pi-4\zeta_0}{4\zeta_0}\right)+\eta_{x^S}^2\int_0^{\omega_0}G^S(\omega,\zeta_0;a_g^s)\,\mathrm{d}\omega. \tag{48}$$

Subsequently, a discretisation of the frequency domain is used to approximate numerically the integral in Eq. (48). Specifically, a uniform frequency grid of N points $\omega_i=\omega_b^l+(i-0.5)\Delta\omega$ with $\omega_i\in(\omega_b^l,\omega_b^u)$ $(i=1,2,\ldots,N)$ is constructed, yielding [72, 3]

$$G^S(\omega_i,\zeta_0;a_g^s)= \begin{cases} 0, & \omega_i\le\omega_b^l \\ \frac{4\zeta_0}{\omega_i\pi-4\zeta_0\omega_{i-1}}\left(\frac{\left(S^S(\omega_i,\zeta_0;a_g^s)\right)^2}{\eta_{x^S}^2}-\Delta\omega\sum_{k=1}^{i-1}G^S(\omega_k,\zeta_0;a_g^s)\right), & \omega_b^l<\omega_i<\omega_b^u \end{cases} \tag{49}$$

The ordinates of the power spectrum $G^S(\omega_i,\zeta_0;a_g^s)$ are determined by recursively applying Eq. (49) $(i=1,2,\ldots,N)$.

Having $G^S(\omega,\zeta_0;a_g^s)$ determined in the range (ω_b^l,ω_b^u), the spectral representation method is applied to generate an ensemble of realisations for estimating the jth non-stationary acceleration time-history. This is done based on [73]

$$\ddot{x}_g^{(j)}(t)=a\ddot{x}_g^R(t)+\varphi(t)\sum_{i=1}^{N_a}\sqrt{4G^S(i\Delta\omega,\zeta_0;a_g^s)\Delta\omega}\cos\left(i\Delta\omega t+\theta_i^{(j)}\right), \tag{50}$$

where $\theta_i^{(j)}$ denotes the independent random phases which are uniformly distributed in the interval $[0,2\pi)$, and N_a is the total number of harmonics considered. The EPS $G(\omega,\zeta_0,t;a_g^s)$ corresponding to the non-stationary stochastic excitation process $\ddot{x}_g(t)$ has two components, namely

$$G(\omega,\zeta_0,t;a_g^s)=a^2G^R(\omega,\zeta_0,t;a_g^s)+\varphi(t)^2G^S(\omega,\zeta_0;a_g^s), \tag{51}$$

where $G^R(\omega,\zeta_0,t;a_g^s)$ is the non-separable EPS and $G^S(\omega,\zeta_0;a_g^s)$ is the time-modulated separable power spectrum of the corrective term. The former can be readily determined by various techniques [74, 75, 76]. Lastly, an iterative scheme is utilised for improving the matching of $G^S(\omega,\zeta_0;a_g^s)$ with the target pseudo-acceleration response spectrum. That is,

$$G^{S(k)}(\omega,\zeta_0;a_g^s)=G^{S(k-1)}(\omega,\zeta_0;a_g^s)\left[\frac{S\left(\omega,\zeta_0;a_g^s\right)^2}{\tilde{S}^{(k-1)}\left(\omega,\zeta_0;a_g^s\right)^2}\right], \tag{52}$$

where $\tilde{S}^{(k)}(\omega, \zeta_0; a_g^s)$ denotes the mean response spectrum of the non-stationary stochastic excitation process $\ddot{x}_g(t)$ at a specific level of peak ground acceleration a_g^s in the kth iteration.

B Eurocode 8 design spectrum

The Eurocode 8 outlines the elastic pseudo-acceleration response spectrum for linear oscillators, characterised by a damping ratio ζ and natural period $T = 2\pi/\omega$ through the following expressions [77]

$$S(T, \zeta, a_g^s) = a_g^s \times \begin{cases} S\left[1 + \frac{T}{T_B}(2.5\eta - 1)\right], & 0 \leq T \leq T_B \\ 2.5S\eta, & T_B \leq T \leq T_C \\ 2.5S\eta\frac{T_C}{T}, & T_C \leq T \leq T_D \\ 2.5S\eta\frac{T_C T_D}{T^2}, & T_D \leq T \leq T_E \\ S\frac{T_C T_D}{T^2}\left[2.5\eta + \frac{T - T_E}{T_F - T_E}(1 - 2.5\eta)\right], & T_E \leq T \leq T_F \\ S\frac{T_C T_D}{T^2}, & T_F \leq T \end{cases}, \tag{53}$$

with

$$\eta = \sqrt{\frac{10}{5 + \zeta}} \geq 0.55, \tag{54}$$

where a_g^s is the peak ground acceleration, S is a soil-dependent amplification factor, and T_B, T_C, T_D, T_E and T_F correspond to the soil-dependent corner periods. For the case of soil type B: $S = 1.20, T_B = 0.15, T_C = 0.5, T_D = 2.0, T_E = 5.0, T_F = 10$.

C Bilinear hysteretic system comprising fractional derivative terms

The herein study considers an SDOF system exhibiting bilinear hysteretic behaviour endowed with fractional derivative elements. In this regard, the restoring force of the system in Eq. (1) is given by

$$g(t, x(t), \dot{x}(t)) = \gamma\omega_0^2 x(t) + (1 - \gamma)\omega_0^2 x_y z(t), \tag{55}$$

with γ denoting the post-yield to pre-yield stiffness ratio and x_y representing the critical value at which yielding occurs; z accounts for a state variable

such that

$$x_y\dot{z}(t) = \dot{x}\left[1 - H(\dot{x}(t))H\left(z(t)-1\right) - H(-\dot{x}(t))H(-z(t)-1)\right], \tag{56}$$

where $H(\cdot)$ is the Heaviside step function.

Following the stochastic linearization and averaging treatments presented in Section 2.2, the equivalent linear elements in Eqs (9) and (11) become

$$\beta(A(t)) = \frac{(1-\gamma)\omega_0^2 S_0(A)}{A\omega(A)} + \frac{\beta}{\omega^{1-\alpha}(A)}\sin\left(\frac{\alpha\pi}{2}\right) - \beta_0 \tag{57}$$

and

$$\omega^2(A(t)) = \omega_0^2\left[\gamma + \frac{(1-\gamma)F_0(A)}{A} + \beta\omega^{\alpha}(A)\cos\left(\frac{\alpha\pi}{2}\right)\right], \tag{58}$$

respectively, where

$$S_0(A(t)) = \begin{cases} \frac{4x_y}{\pi}\left(1-\frac{x_y}{A}\right), & A > x_y \\ 0, & A \le x_y \end{cases} \tag{59}$$

$$F_0(A(t)) = \begin{cases} \frac{A}{\pi}\left[\Lambda - \frac{1}{2}\sin(2\Lambda)\right], & A > x_y \\ A, & A \le x_y \end{cases}, \tag{60}$$

with $\cos(\Lambda) = 1 - \frac{2x_y}{A}$. Next, considering Eqs. (57) and (58), Eqs. (13) and (14) lead to fragkoulis2019non,kougioumtzoglou2022approximate

$$\begin{aligned} \beta_{eq}(c(t)) =& -\beta_0 + \frac{J\beta\sin(\frac{\alpha\pi}{2})}{c(t)}\int_0^{\infty}\frac{A}{\omega^{1-\alpha}(A)}\exp\left(-\frac{JA^2}{2c(t)}\right)\mathrm{d}A \\ &+ \frac{4Jx_y\omega_0^2(1-\gamma)}{\pi c(t)}\int_{x_y}^{\infty}\frac{1-\frac{x_y}{A}}{\omega(A)}\exp\left(-\frac{JA^2}{2c(t)}\right)\mathrm{d}A \end{aligned} \tag{61}$$

and

$$\begin{aligned} \omega_{eq}^2(c(t)) =& \omega_0^2 - (1-\gamma)\omega_0^2\left[\exp\left(-\frac{Jx_y^2}{2c(t)}\right)\right. \\ &\left. - \frac{J}{\pi c(t)}\int_{x_y}^{\infty}(\Lambda - \frac{1}{2}\sin(2\Lambda))A\exp\left(-\frac{JA^2}{2c(t)}\right)\mathrm{d}A\right] \\ &+ \frac{J\beta\cos(\frac{\alpha\pi}{2})}{c(t)}\int_0^{\infty}\omega^{\alpha}(A)A\exp\left(-\frac{JA^2}{2c(t)}\right)\mathrm{d}A, \end{aligned} \tag{62}$$

respectively.

References

[1] A. Giaralis, P. D. Spanos, Effective linear damping and stiffness coefficients of nonlinear systems for design spectrum based analysis, Soil Dynamics and Earthquake Engineering 30 (9) (2010) 798–810.

[2] I. P. Mitseas, I. A. Kougioumtzoglou, A. Giaralis, M. Beer, A novel stochastic linearization framework for seismic demand estimation of hysteretic MDOF systems subject to linear response spectra, Structural Safety 72 (2018) 84–98.

[3] I. P. Mitseas, M. Beer, Modal decomposition method for response spectrum based analysis of nonlinear and non-classically damped systems, Mechanical Systems and Signal Processing 131 (2019) 469–485.

[4] Y. Jiang, X. Zhang, M. Beer, H. Zhou, Y. Leng, An efficient method for reliability-based design optimization of structures under random excitation by mapping between reliability and operator norm, Reliability Engineering & System Safety 245 (2024) 109972.

[5] I. P. Mitseas, I. A. Kougioumtzoglou, P. D. Spanos, M. Beer, Nonlinear MDOF system survival probability determination subject to evolutionary stochastic excitation, Strojniski Vestnik-Journal of Mechanical Engineering 62 (7-8) (2016) 440–451.

[6] P. Ni, V. Fragkoulis, F. Kong, I. Mitseas, M. Beer, Non-stationary response of nonlinear systems with singular parameter matrices subject to combined deterministic and stochastic excitation, Mechanical Systems and Signal Processing 188 (2023) 110009.

[7] J. A. T. M. J. Sabatier, O. P. Agrawal, J. A. T. Machado, Advances in fractional calculus, Vol. 4(9), Springer, 2007.

[8] J. T. Machado, V. Kiryakova, F. Mainardi, Recent history of fractional calculus, Communications in Nonlinear Science and Numerical Simulation 16 (3) (2011) 1140–1153.

[9] A. Pirrotta, I. A. Kougioumtzoglou, A. Di Matteo, V. C. Fragkoulis, A. A. Pantelous, C. Adam, Deterministic and random vibration of linear systems with singular parameter matrices and fractional derivative terms, Journal of Engineering Mechanics 147 (6) (2021) 04021031.

[10] Y. Zhang, I. A. Kougioumtzoglou, F. Kong, A Wiener path integral technique for determining the stochastic response of nonlinear oscillators with fractional derivative elements: A constrained variational formulation with free boundaries, Probabilistic Engineering Mechanics 71 (2023) 103410.

[11] A. Di Matteo, P. D. Spanos, Determination of nonstationary stochastic response of linear oscillators with fractional derivative elements of rational order, Journal of Applied Mechanics (2023) 1–25.

[12] D. Jerez, V. Fragkoulis, P. Ni, I. Mitseas, M. A. Valdebenito, M. G. Faes, M. Beer, Operator norm-based determination of failure probability of nonlinear oscillators with fractional derivative elements subject to imprecise stationary gaussian loads, Mechanical Systems and Signal Processing 208 (2024) 111043.

[13] Y. A. Rossikhin, M. V. Shitikova, Applications of fractional calculus to dynamic problems of linear and nonlinear hereditary mechanics of solids, Applied Mechanics Reviews 50 (1997) 15–67.

[14] Y. A. Rossikhin, M. V. Shitikova, Application of fractional calculus for dynamic problems of solid mechanics: novel trends and recent results, Applied Mechanics Reviews 63 (1) (2010).

[15] N. Makris, G. F. Dargush, M. C. Constantinou, Dynamic analysis of generalized viscoelastic fluids, Journal of Engineering Mechanics 119 (8) (1993) 1663–1679.

[16] M. Di Paola, G. Failla, A. Pirrotta, A. Sofi, M. Zingales, The mechanically based non-local elasticity: an overview of main results and future challenges, Philosophical Transactions of the Royal Society A: Mathematical, Physical and Engineering Sciences 371 (1993) (2013) 20120433.

[17] K. J. Papoulia K.D., Visco-hyperelastic model for filled rubbers used in vibration isolation, J. Eng. Mater. Technol. 119 (1997) 292–297.

[18] A. Di Matteo, F. L. Iacono, G. Navarra, A. Pirrotta, Innovative modeling of tuned liquid column damper motion, Communications in Nonlinear Science and Numerical Simulation 23 (1-3) (2015) 229–244.

[19] C. G. Koh, J. M. Kelly, Application of fractional derivatives to seismic analysis of base-isolated models, Earthquake Engineering & Structural Dynamics 19 (2) (1990) 229–241.

[20] N. Makris, M. C. Constantinou, Fractional-derivative Maxwell model for viscous dampers, Journal of Structural Engineering 117 (9) (1991) 2708–2724.

[21] A. A. Markou, G. D. Manolis, A fractional derivative zener model for the numerical simulation of base isolated structures, Bullettin of Earthquake Engineering 14 (2016) 283–295.

[22] H. Li, D. Gomez, S. J. Dyke, Z. Xu, Fractional differential equation bearing models for base-isolated buildings: Framework development, Journal of Structural Engineering 146 (2020). doi:https://doi.org/10.1061/(ASCE)ST.1943-541X.0002508.

[23] F. Rüdinger, Tuned mass damper with fractional derivative damping, Engineering Structures 28 (13) (2006) 1774–1779.

[24] J. Xu, J. Li, Stochastic dynamic response and reliability assessment of controlled structures with fractional derivative model of viscoelastic dampers, Mechanical Systems and Signal Processing 72 (2016) 865–896.

[25] K. R. dos Santos, J. G. Duarte, Stochastic response determination of hysteretic vibratory energy harvesters with fractional derivatives via stochastic averaging, Journal of Engineering Mechanics 150 (7) (2024) 04024035.

[26] Y.-H. Sun, Y. Sun, Y.-G. Yang, W. Xu, Bifurcation and stability analysis of a hybrid energy harvester with fractional-order proportional–integral–derivative controller and gaussian white noise excitations, Probabilistic Engineering Mechanics 73 (2023) 103464.

[27] I. A. Kougioumtzoglou, P. Ni, I. P. Mitseas, V. C. Fragkoulis, M. Beer, An approximate stochastic dynamics approach for design spectrum based response analysis of nonlinear structural systems with fractional derivative elements, International Journal of Non-Linear Mechanics 146 (2022) 104178.

[28] H. H. Lee, C.-S. Tsai, Analytical model of viscoelastic dampers for seismic mitigation of structures, Computers & Structures 50 (1) (1994) 111–121.

[29] F. Kong, Y. Zhang, Y. Zhang, Non-stationary response power spectrum determination of linear/non-linear systems endowed with fractional derivative elements via harmonic wavelet, Mechanical Systems and Signal Processing 162 (2022) 108024.

[30] M. P. Singh, T.-S. Chang, H. Nandan, Algorithms for seismic analysis of mdof systems with fractional derivatives, , Engineering Structures 33 (2011) 2371–2381.

[31] R. Lewandowski, Z. Pawlak, Dynamic analysis of frames with viscoelastic dampers modeled by rheological models with fractional derivatives, Journal of Sound and Vibration 330 (2011) 923–936.

[32] A. Aprile, J. A. Inaudi, J. M. Kelly, Evolutionary model of viscoelastic dampers for structural applications, Journal of Engineering Mechanics 123 (1997) 551–560.

[33] E. Tubaldi, M. Barbato, A. Dall'Asta, Performance-based seismic risk assessment for buildings equipped with linear and nonlinear viscous dampers, Engineering Structures 78 (2014) 90–99.

[34] I. P. Mitseas, I. A. Kougioumtzoglou, M. Beer, An approximate stochastic dynamics approach for nonlinear structural system performance-based multi-objective optimum design, Structural Safety 60 (2016) 67–76.

[35] D. Vamvatsikos, C. A. Cornell, Incremental dynamic analysis, Earthquake Engineering & Structural Dynamics 31 (3) (2002) 491–514.

[36] D. Vamvatsikos, Performing incremental dynamic analysis in parallel, Computers & Structures 89 (1-2) (2011) 170–180.

[37] I. P. Mitseas, M. Beer, First-excursion stochastic incremental dynamics methodology for hysteretic structural systems subject to seismic excitation, Computers & Structures 242 (2021) 106359.

[38] B. Chen, C. Li, B. Wilson, Y. Huang, Fractional modeling and analysis of coupled MR damping system, IEEE/CAA Journal of Automatica Sinica 3 (2016) 288–294.

[39] P. Cacciola, A stochastic approach for generating spectrum compatible fully nonstationary earthquakes, Computers & Structures 88 (15-16) (2010) 889–901.

[40] A. Giaralis, P. Spanos, Wavelet-based response spectrum compatible synthesis of accelerograms-Eurocode application (EC8), Soil Dynamics and Earthquake Engineering 29 (1) (2009) 219–235.

[41] D. D. Pfaffinger, Calculation of power spectra from response spectra, Journal of Engineering Mechanics 109 (1) (1983) 357–372.

[42] P. D. Spanos, L. M. V. Loli, A statistical approach to generation of design spectrum compatible earthquake time histories, International Journal of Soil Dynamics and Earthquake Engineering 4 (1) (1985) 2–8.

[43] J. T. Christian, Generating seismic design power spectral density functions, Earthquake Spectra 5 (2) (1989) 351–368.

[44] Y. J. Park, New conversion method from response spectrum to PSD functions, Journal of Engineering Mechanics 121 (12) (1995) 1391–1392.

[45] I. D. Gupta, M. D. Trifunac, Defining equivalent stationary PSDF to account for nonstationarity of earthquake ground motion, Soil Dynamics and Earthquake Engineering 17 (2) (1998) 89–99.

[46] M. Shields, Simulation of spatially correlated nonstationary response spectrum–compatible ground motion time histories, Journal of Engineering Mechanics 141 (6) (2015) 04014161.

[47] P. T. Brewick, M. Hernandez-Garcia, S. F. Masri, A. W. Smyth, A data-based probabilistic approach for the generation of spectra-compatible time-history records, Journal of Earthquake Engineering 22 (8) (2018) 1365–1391.

[48] J. B. Roberts, P. D. Spanos, Random vibration and statistical linearization, Courier Corporation, 2003.

[49] J. B. Roberts, P. D. Spanos, Stochastic averaging: an approximate method of solving random vibration problems, International Journal of Non-Linear Mechanics 21 (2) (1986) 111–134.

[50] I. A. Kougioumtzoglou, P. D. Spanos, An approximate approach for nonlinear system response determination under evolutionary stochastic excitation, Current science (2009) 1203–1211.

[51] P. D. Spanos, A. Di Matteo, Y. Cheng, A. Pirrotta, J. Li, Galerkin scheme-based determination of survival probability of oscillators with fractional derivative elements, Journal of Applied Mechanics 83 (12) (2016).

[52] V. C. Fragkoulis, I. A. Kougioumtzoglou, A. A. Pantelous, M. Beer, Non-stationary response statistics of nonlinear oscillators with fractional derivative elements under evolutionary stochastic excitation, Nonlinear Dynamics 97 (4) (2019) 2291–2303.

[53] V. C. Fragkoulis, I. A. Kougioumtzoglou, Survival probability determination of nonlinear oscillators with fractional derivative elements under evolutionary stochastic excitation, Probabilistic Engineering Mechanics 71 (2023) 103411.

[54] M. Abramowitz, I. A. Stegun, Handbook of Mathematical Functions with Formulas, Graphs, and Mathematical Tables, Vol. 55, US Government printing office, 1964.

[55] P.-T. D. Spanos, G. P. Solomos, Markov approximation to transient vibration, Journal of Engineering Mechanics 109 (4) (1983) 1134–1150.

[56] G. P. Solomos, P. T. D. Spanos, Oscillator response to nonstationary excitation, Journal of Applied Mechanics 51 (1984) 907–912.

[57] P. D. Spanos, I. A. Kougioumtzoglou, Survival probability determination of nonlinear oscillators subject to evolutionary stochastic excitation, Journal of Applied Mechanics 81 (5) (2014) 051016.

[58] I. P. Mitseas, I. A. Kougioumtzoglou, P. D. Spanos, M. Beer, Reliability assessment of nonlinear MDOF systems subject to evolutionary stochastic excitation, in: Proceedings of the 7th International Conference on

Computational Stochastic Mechanics (CSM7), Santorini, Greece, Research Publishing, 2014, pp. 420–431, ISBN: 978-981-09-5348-5.

[59] M. B. Priestley, Evolutionary spectra and non-stationary processes, Journal of the Royal Statistical Society: Series B (Methodological) 27 (2) (1965) 204–229.

[60] R. Dahlhaus, Fitting time series models to nonstationary processes, The annals of Statistics 25 (1) (1997) 1–37.

[61] P.-T. D. Spanos, L. D. Lutes, Probability of response to evolutionary process, Journal of the Engineering Mechanics Division 106 (2) (1980) 213–224.

[62] I. P. Mitseas, M. Beer, Fragility analysis of nonproportionally damped inelastic MDOF structural systems exposed to stochastic seismic excitation, Computers & Structures 226 (2020) 106129.

[63] B. Ellingwood, Earthquake risk assessment of building structures, Reliability Engineering & System Safety 74 (2001) 251–262.

[64] H. A. Jensen, F. Mayorga, M. A. Valdebenito, On the reliability of structures equipped with a class of friction-based devices under stochastic excitation, Computer Methods in Applied Mechanics and Engineering 364 (112965) (2020).

[65] S. Au, J. L. Beck, First excursion probabilities for linear systems by very efficient importance sampling, Probabilistic Engineering Mechanics 16 (2001) 193–207.

[66] M. Grigoriu, Do seismic intensity measures (IMs) measure up?, Probabilistic Engineering Mechanics 46 (2016) 80–93.

[67] J. Liang, S. R. Chaudhuri, M. Shinozuka, Simulation of nonstationary stochastic processes by spectral representation, Journal of Engineering Mechanics 133 (6) (2007) 616–627.

[68] G. P. Solomos, P.-T. D. Spanos, Structural reliability under evolutionary seismic excitation, Soil Dynamics and Earthquake Engineering 2 (2) (1983) 110–116.

[69] P. C. Jennings, Equivalent viscous damping for yielding structures, Journal of the Engineering Mechanics Division 94 (1) (1968) 103–116.

[70] R. Husid, Características de terremotos. análisis general, Revista IDIEM 8 (1) (1969) ág–21.

[71] E. H. Vanmarcke, Structural response to earthquakes, in: Developments in Geotechnical Engineering, Vol. 15, Elsevier, 1976, pp. 287–337.

[72] P. Cacciola, P. Colajanni, G. Muscolino, Combination of modal responses consistent with seismic input representation, Journal of Structural Engineering 130 (1) (2004) 47–55.

[73] M. Shinozuka, G. Deodatis, Simulation of stochastic processes by spectral representation, Applied Mechanics Reviews 44 (4) (1991) 191–204.

[74] L. Cohen, Time-frequency distributions-a review, Proceedings of the IEEE 77 (7) (1989) 941–981.

[75] J. P. Conte, B.-F. Peng, An explicit closed-form solution for linear systems subjected to nonstationary random excitation, Probabilistic Engineering Mechanics 11 (1) (1996) 37–50.

[76] P. D. Spanos, G. Failla, Evolutionary spectra estimation using wavelets, Journal of Engineering Mechanics 130 (8) (2004) 952–960.

[77] CEN, Eurocode 8: Design of Structures for Earthquake Resistance - Part 1: General Rules, Seismic Actions and Rules for Buildings, Comité Européen de Normalisation, Brussels EN 1998-1: 2003 E. (2004).